The 14th International Topical Meeting on Nuclear Reactor Thermalhydraulics, NURETH-14
Toronto, Ontario, Canada, September 25-30, 2011

NURETH14-467

EXPERIMENTAL STUDIES ON HEAT TRANSFER IN EXTERNAL COOLING OF THE REACTOR PRESSURE VESSEL

T. Merisaari[1], H. Purhonen[2], A. Räsänen[2], R. Kyrki-Rajamäki[2], K. Myllymäki[3] and T. Toppila [3]
[1] TVO, Finland
[2] Lappeenranta University of Technology, Lappeenranta, Finland
[3] Fortum Power and Heat, Finland

Abstract

The filling of the reactor cavity by accidental initiation of the containment spray system, while reactor is in full power, could have severe consequences. If the relatively cold water suddenly cools down the wall of fully pressurized reactor pressure vessel and a crack is assumed to be located on the outer surface of the vessel, the induced thermal stresses might damage the pressure vessel wall. The effects of the inadvertent cooling and pressurized thermal shock (PTS) were studied experimentally at Lappeenranta University of Technology and the heat transfer coefficients gained from the experimental results were compared with calculations.

Introduction

To accurately estimate the effect of the external cooling on the pressure vessel for Loviisa NPP, a VVER-440 type reactor, the effects of the inadvertent cooling were studied experimentally and the heat transfer from the reactor pressure vessel wall to the coolant outside was defined. This study concentrated in the phenomena in the surface heat transfer that have effect on the PTS, thus the rapid changes in the heat transfers are out of the focus due to the time constant of the massive steel structure. The experimental results were compared with calculations using different heat transfer correlations.

In the test arrangement a rectangular steel bar that had heaters on one side was enclosed in a flow channel on the opposite side. The steel bar and the flow channel represent a 100 mm wide section of the pressure vessel wall and the reactor cavity flow channel. Instrumentation was designed in order to define the heat transfer coefficient on the wall surface. However, as measuring of the surface temperature is not straightforward, an inverse script was applied to the measured data to estimate the surface temperature.

1. Design of the test facility

The main focus was on the areas of the wall structure with high radiation in the real NPP. Since the pressure vessel is axially symmetric at reactor level, the geometry can be represented with a sector of the pressure vessel wall and the corresponding part of the reactor cavity as long as the heat transfer through the sides is negligible. Further, because the radius of the wall is significantly greater than the thickness of the wall, the curvature can be ignored and the sector replaced with a rectangular shape.

The main component in the setup was a rectangular steel bar that had heaters on one side and was enclosed in a flow channel on the opposite side, Figure 1. Depth of the bar was the same as wall thickness of the pressure vessel. The bar was tried to make high enough to observe relevant vertical phenomena in the flow channel. Width was chosen to be large enough to control the effects of boundaries on heat transfer. The material used was low alloy steel with heat transfer properties close to the steel used in the pressure vessel. The stainless steel liner was omitted from the setup. The liner would have insignificant effect on cooling of the outer surface. Surface of the bar was machined and coated with anti-corrosion paint similar to the one used in the pressure vessel. The outside of the test rig was mostly insulated with mineral wool.

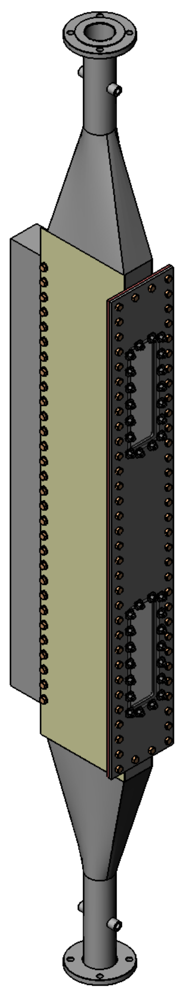

Figure 1 Test section of the facility representing the pressure vessel wall and the flow channel in the reactor cavity.

The flow channel was made from steel plates, sidewalls were 4 mm and front wall was 8 mm thick. The front wall and steel bar were attached to the channel with bolts. Holes for the bolts were oversized to allow the bar to bend under uneven thermal loading without breaking the channel. The parts were thermally insulated from each other with 1.5 mm PTFE sheet. The same L-shaped PTFE sheet extends to the other side of the flow channel and was bent between the side walls and front wall of the channel.

To achieve an even velocity profile in the flow channel in the experimental setup, the channel was connected to the pipelines with an expansion at the inlet and a reduction at the outlet. Height of the straight part was also extended both up and down to allow the flow to stabilize. There was a perforated metal plate inside the inlet expansion, which prevented splashes and evened out the velocity profile. There were two windows in the front wall for visual observations. Process chart of the test rig is presented in Figure 2.

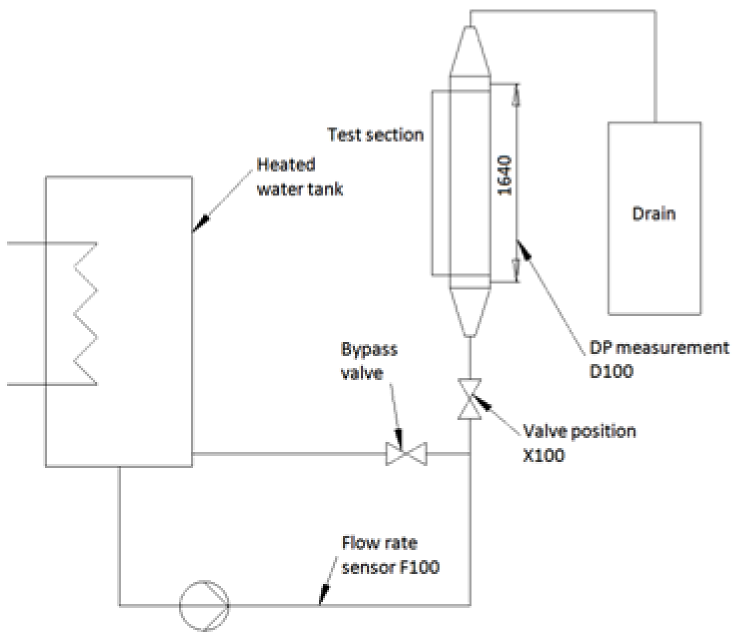

Figure 2 Process chart showing components and auxiliary measurements.

The heater element was made of six 8.5 mm diameter rods rated 1 kW each. Total length of a rod was 1600 mm but both ends had 50 mm non-heated sections for electrical wiring. The rods were installed inside slots machined on an aluminium plate. The aluminium plate was attached with bolts to the steel bar with the heater rods facing the steel wall, Figure 3. Thermocouple positions are shown in Figure 4. Locations of the thermocouples T206, T209, T231 and T234 are off the centerline. Thermocouples T117, T118 and T119 are positions in machined slots on the surface and the edges of the slots are bent over the thermocouple wires.

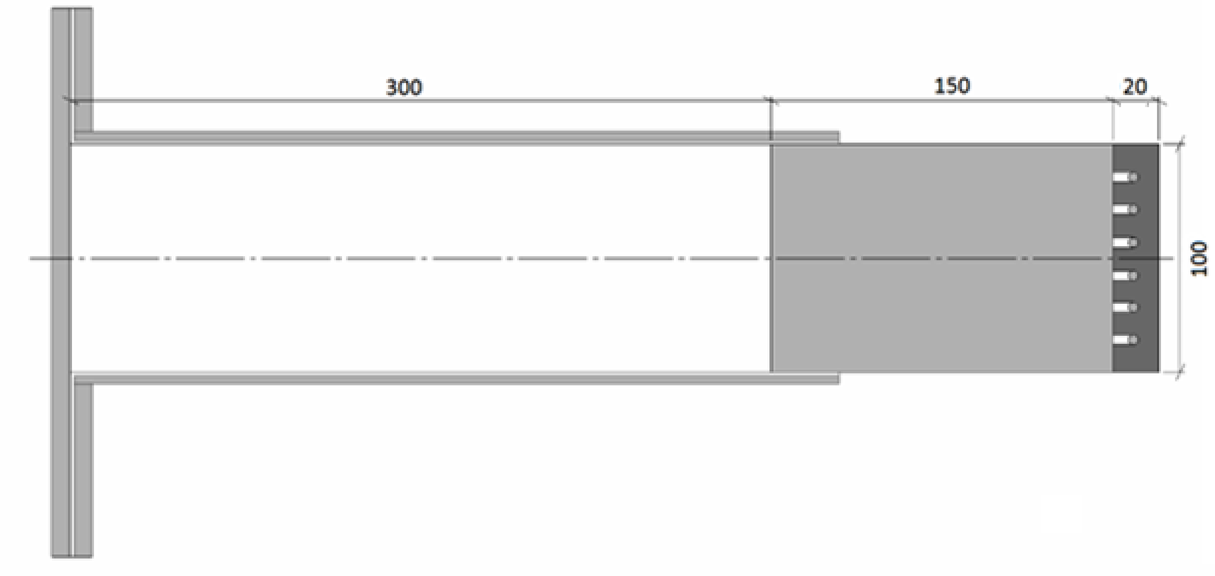

Figure 3   Cross section of the test rig showing (from the left) the front wall, flow channel, steel bar, and plate with heaters.

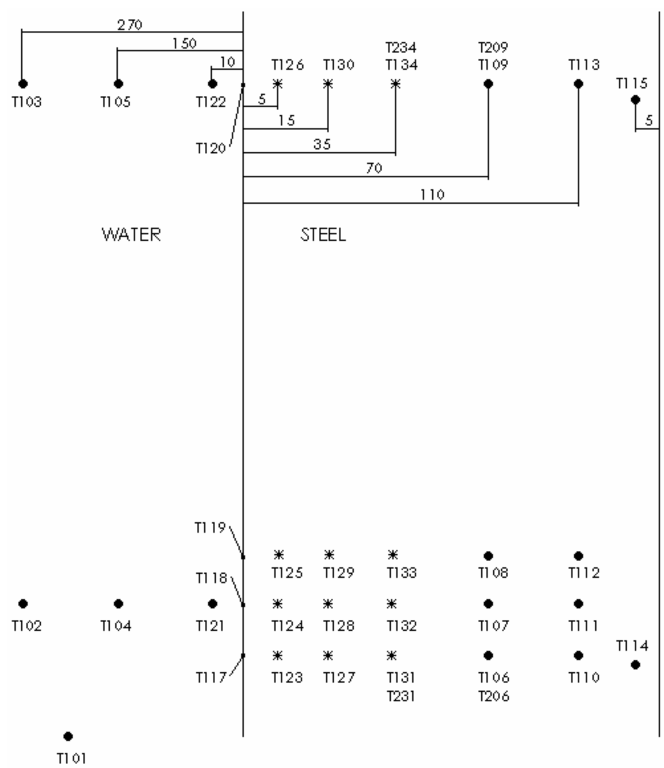

Figure 4   Thermocouple positions in the centerline of the test section.

2. Instrumentation and measuring system

The main measurements consisted of 26 thermocouples measuring temperatures from inside the steel bar, six measuring water temperatures in the channel and two measuring temperatures from the channel inlet and flow meter. Water flow rate was monitored by a flow meter and water level by a differential pressure sensor. The controlling parameter was flow rate rather than the water level rise velocity.

Thermocouples were K-type with 3 mm or 1 mm outer diameter. Temperature change was anticipated to be especially fast near the surface, so smaller diameter thermocouples with shorter time constant were used there. In order to make installation easier and improve contact the 1 mm thermocouples were soldered inside 3 mm steel sleeves. Four of the 1 mm measurements were installed in slots machined on the surface. These thermocouples measure temperature very close to the surface. Edges of the slots were carefully bent over the thermocouple wires. The response time of the thermocouples was partly handled inherently by the inverse calculation method.

The thermocouples were installed in different elevations in order to observe how temperature change of water affects heat transfer. The upper measurement consisted of six thermocouples in a one dimensional arrangement. The lower cluster is arranged in a two dimensional grid with thermocouples in three rows. Temperature data from the two additional rows could be used as boundary conditions for the center row.

The main measuring system was a combo system, consisting of a rack, A/D converter and two multiplexer modules which also contained channel-specific instrumentation amplifiers and cold junction compensation temperature measurements for the thermocouples. The rack was connected to a data storing PC-computer with a fiber-optic link. The system used an internal thermocouple measurement mode, which utilizes channel specific instrumentation amplifiers. Cold junction compensation and linearization were also handled by the measurement system. Channel specific gain and offset errors were measured using a calibrated voltage reference calibrator. The flow meter and the differential pressure measurement output 4-20 mA current signals, which were converted to voltage signals by 250 Ω resistors with specific accuracy of 0.1 %.

The data feed from the main measurement system was recorded 25 times per second. As the measurement frequency was set to 5000 Hz, each recorded measurement point was the average of 200 points. This averaging was done to reduce the random noise in the measurements.

2.1 Thermocouple accuracy

Since the accuracy of temperature measurements was paramount for the tests, some additional steps were taken to make sure that the data would be as accurate as possible. The thermocouples used can have errors up to ±1.5 °C in temperatures up to 400 °C. The normal procedure is to test the thermocouples at 95 °C in a water bath. Since the temperatures used in these experiments were much higher, the true S-curve of the thermocouples was measured.

A special test rig with 40 kg of electrolytic copper in a well insulated enclosure was fabricated. Holes were drilled to the copper in order to get the thermocouples to the same temperature as the copper. To measure the true temperature of the copper block, a calibrated PT-100 probe was used to measure the temperature during the cooling of the block and the thermocouples were checked against the PT-100 probe. The test lasted little over 24 hours, in this time the temperature of the copper block decreased from 270 to 90 °C. Since thermal conductivity of copper is about 400 W/m°C, the temperature distribution inside the block was considered uniform.

2.2 Data handling procedure

It was clear that the raw temperature data had to be processed some way to get a more accurate result, since small temperature differences would be used to calculate results. Individual correction of measurement channels was discarded as unreliable and instead two different groups of thermocouples were identified. The following scheme was implemented:

- Correct individual offset errors by fixing the measurement channels to their 95 ºC liquid bath test points.
- Calculate correction polynomials for two different kinds of thermocouple types. Average S-curves used for each group and polynomial curves fitted to data as a function of reference temperature.
- Correct measurement data using the polynomials.

Usually a table of accuracy is provided with the measurement results. Since these accuracy enhancing methods cannot be validated in an acceptable way, the measurement results are provided only without the correction methods applied. Despite this, the corrected values are the best estimate that can be given using the available resources.

Because of the uncertainty associated with the enhancement, the overall accuracy of temperature measurement is at least ± 1.8 ºC for the measurement system.

3. Calculation of heat transfer coefficient

Heat transfer coefficient is a factor used to describe magnitude of convective heat transfer. The coefficient is usually derived from correlations that have fairly limited areas of application. It can be solved by rearranging Newton's law of cooling

$$h = \frac{q''}{(T_s - T_\infty)} \tag{1}$$

T_s surface temperature
T_∞ free stream temperature of fluid; boiling point if the surface temperature is high enough
q" heat flux from the wall to the water

It is obvious that boiling and ordinary convection have very different coefficients. It is also difficult to tell exactly when heat transfer changes from boiling to convection. The transition is therefore neglected and water temperature from mid channel measurement is used as the free stream temperature for the whole range.

The other two variables in the equation also proved to be difficult to find out. It is not possible to accurately measure surface temperature of a submerged object. The measurement device would typically alter the real temperature to such degree, that measurement is no longer meaningful. If the surface temperature was known, heat flux could be determined from the one dimensional conduction law

$$q'' = k\frac{dT}{dx} \approx k\frac{(T_s - T_{in})}{\Delta x} \tag{2}$$

k	heat conductivity
T_{in}	internal temperature
Δx	distance of internal temperature measurement point from surface

Once the surface starts to cool, high heat capacity and limited conductivity of the bar cause the temperature distribution to be non linear. As a consequence the discrete form of the conduction law only applies with very small values of Δx. This could be countered by moving the measurement points tighter together, but the problem with closely spaced thermocouples is that the temperature difference between them is small compared to the accuracy of the sensor. This would lead to very large errors.

3.1 Inverse calculation

The surface heat flux and temperature can be simultaneously solved using inverse calculation. Here the function specification method is used. Only a short description of the method is given here. More comprehensive information on the method can be found in literature [1, 2].

First step is to prepare a numeric model (finite difference method is used in this case) to solve a time dependent conduction problem in the desired geometry. Then a surface heat flux is guessed and the temperature field is solved using the model. The calculated temperature field is compared to the temperature measurements and a correction factor for the heat flux is calculated based on the difference. The procedure is repeated with the new value of heat flux until solution has converged. A new time step is started using the heat flux from the previous step [1].

When an inversion method such as this is used, only the properties that are included in the model are taken into account. For example heat capacity of the steel bar causes temperature variations of the surface to reach the inside measurement points in a damped and delayed form. This behaviour is inherently compensated in the model to some extent. If a transient is very fast, it is completely damped by the bar and no information of it reaches the internal temperature measurements. It is also difficult to include thermocouples in the model because of their small size and complicated internal geometry with regard to numerical model cell size. Therefore the dynamic error of the thermocouples remains in the solution.

Because inverse problems are ill-posed, a small error in the input values could lead to very large errors in the solution. This instability can be alleviated by using future time steps to evaluate present time step. A predefined heat flux must be used for all these time steps. This introduces an error to the estimation, since the predefined value agrees with the real one only in steady state. This error limits the use of stabilization [2]. 3-5 future time steps were used to get a stabilized solution.

A Matlab script using the inverse method was written to analyse the measurement data from the experiments. The quasi two dimensional calculation routine, which outperformed the one dimensional in preliminary tests, proved to be unreliable when real temperature data was used. Therefore the more robust one dimensional script was used to calculate heat transfer coefficient.

3.2 Error estimation

Error estimation for the inverse procedure is troublesome, since the measured values influence the solution indirectly. The estimation is therefore done only for the direct solution. Error limits for the inverse calculation are most likely of the same magnitude.

Estimation was done using the variance method, because it gives a more realistic result when multiple parameters directly affect the result. Averaging is used to reduce the variance of temperature measurements. Variance each parameter or measurement can be written when the limits of values are known.

$$s_x^2 = \frac{a_x^2}{3n} \tag{3}$$

s^2	variance
a	estimated maximum error limit for parameter
x	parameter or measurement
n	number of samples used for averaging

Total variance for heat transfer coefficient is solved from equation

$$s_h^2 = \left|\frac{\partial h}{\partial T_{in}}\right|^2 s_{T_{in}}^2 + \left|\frac{\partial h}{\partial T_\infty}\right|^2 s_{T_{in}}^2 + \left|\frac{\partial h}{\partial T_s}\right|^2 s_{T_s}^2 + \left|\frac{\partial h}{\partial k}\right|^2 s_k^2 + \left|\frac{\partial h}{\partial \Delta x}\right|^2 s_{\Delta x}^2 \tag{4}$$

Total uncertainty corresponding to 95% confidence intervals in a normal distribution is

$$u_h = 2\sqrt{s_h^2} \tag{5}$$

The result is realistic if the maximum error limits are chosen correctly. Accuracy of temperature measurement system is used for T_s, T_{in} and T_∞. Error estimate for Δx was based on diameter of the thermocouple and error for k was estimated based on the temperature variation of thermal conductivity. The dynamic error of thermocouples is still unresolved, but estimates for other errors are present.

4. Test arrangement

The tests were carried out in atmospheric pressure. Flow rate was preset by driving water through the channel while it was still unheated. Nearly constant flow rate during the whole experiment was attained by circulating the water through a bypass line just before the experiment. When the experiment started, the bypass valve was closed and the system line opened allowing water to flow inside the channel. In the transient the water level in the flow channel moves upward according to the used flow rate. As the channel is filled with water, hydrostatic pressure is formed and flow rate drops. Therefore pump speed and valve position were adjusted during the experiment to get a constant flow rate.

Initial surface temperature was approximately 255 °C on the center row in the lower measurement cluster. The top row was at a considerably higher temperature. It was suspected that lack of air circulation in the channel caused the top of the bar to overheat. The back side of the bar was also at a higher temperature than was originally intended. Since the measurement takes place on the front side, it was concluded that it was more important to have a linear radial temperature distribution than the exactly correct back wall temperature.

5. Test results

Once the initial peak caused by bubble boiling passes, coefficient starts to slowly drop towards a constant value. The intense boiling period lasts for only about one second and though the surface cools down very fast in the beginning, the inside remains at a higher temperature, Figure 5. Results are given as graphs that show the beginning of the transient.

An example is showed to present how the coefficients are calculated. First the measurement data are processed as was discussed in section 2.2. Then the inverse script is applied to the data. Estimated surface temperature and heat flux are shown in Figures 6 and 7. Measured temperatures from the middle of the channel are used as free stream temperatures for the temperature difference. Heat transfer coefficients based on these values including results with one of the applied heat transfer correlations are shown in Figure 8.

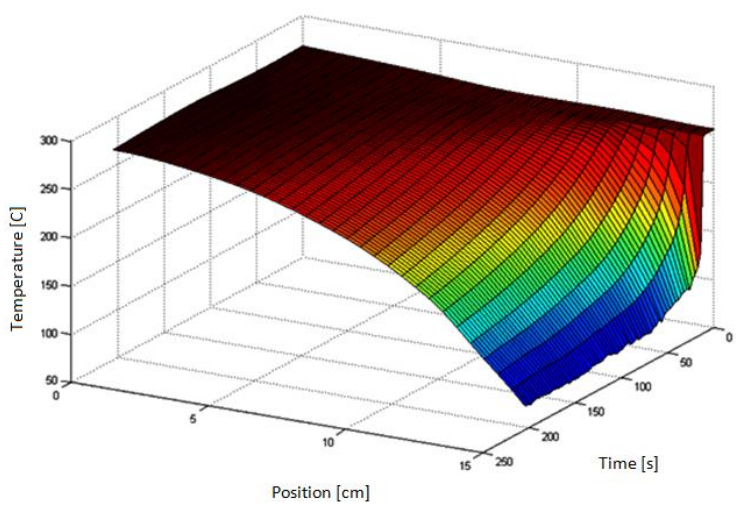

Figure 5 Temperature distribution of the bar during a test. Values are interpolated from the measurements.

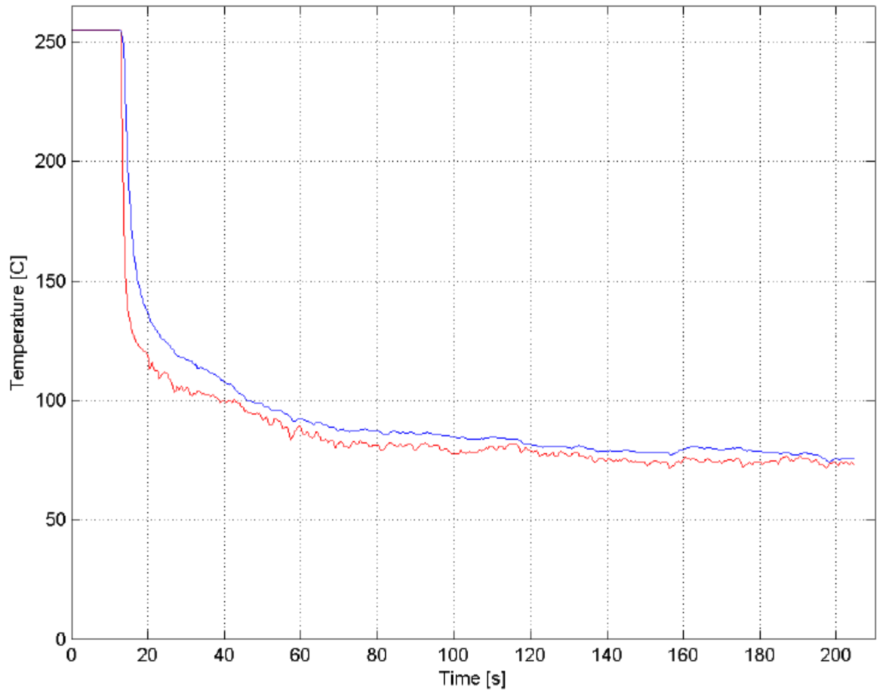

Figure 6   Calculated surface temperatures with surface thermocouple (red) and without (blue).

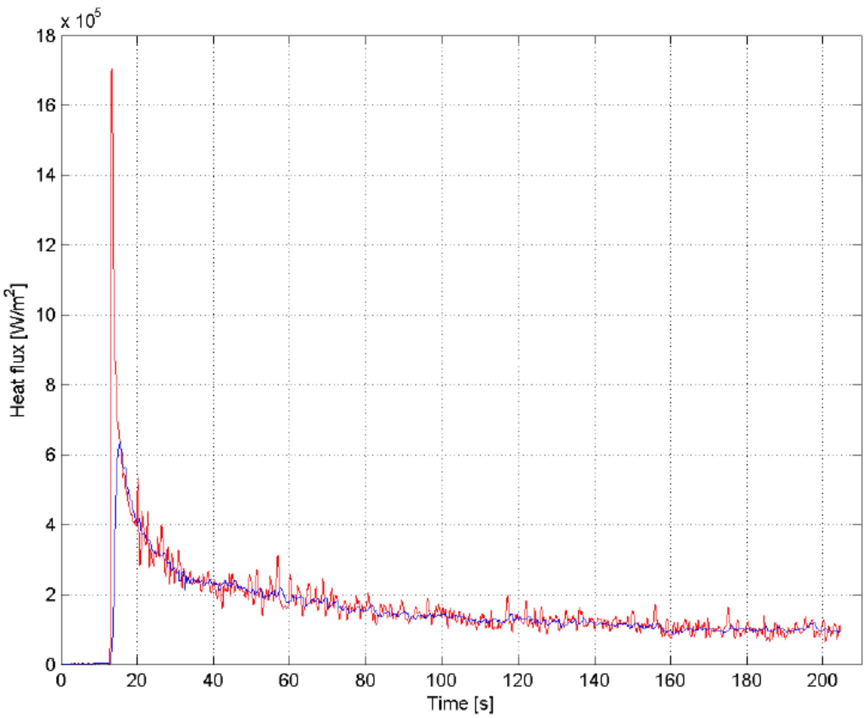

Figure 7   Calculated surface heat flux with surface thermocouple (red) and without (blue).

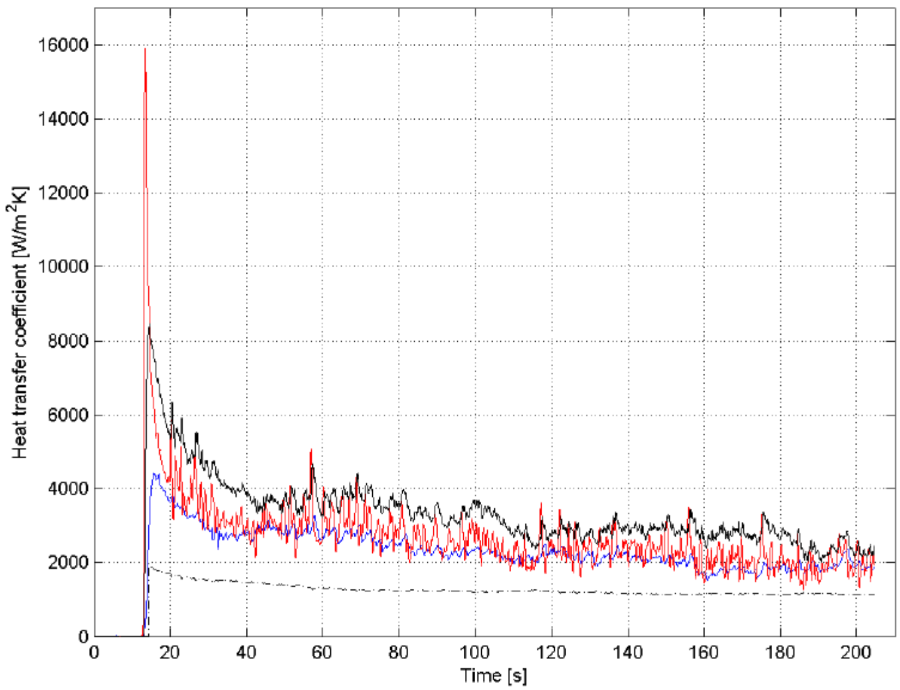

Figure 8 Heat transfer coefficients from test. With surface thermocouple (red), without (blue), directly from measurements (black) and Churchill & Chu correlation (dash line).

The calculation is sensitive to errors in the surface mounted thermocouple. When a steady state calibration was done on the temperature measurements, the surface thermocouple reading was not aligned with the other measurements. It was cooler than it should have been which probably means it has too much contact surface with water. This leads to suspect that the coefficients might be too large in cases where the surface measurements are used. Therefore the calculations were also done using only the internal measurements. Because of impaired transient response, the boiling peak is not fully visible when only internal measurements are used. Both curves are shown along with one using the Churchill & Chu correlation and one solved directly from the measurement data. The correlation value is displayed only for the convection part. Direct solution is calculated using uncorrected measurement data and the following equation [3].

$$q'' = h(T_s - T_\infty) = k\frac{T_s - T_\infty}{\Delta x} \tag{6}$$

T_s	surface temperature
T_∞	free stream temperature of fluid; boiling point if the surface temperature is high enough
q"	heat flux from the wall to the water
k	heat conductivity
Δx	distance of internal temperature measurement point from surface

6. Summary

The reactor pressure vessels in Loviisa NPP are equipped with external cooling systems that flood the reactor cavity with water. The filling of the reactor cavity by accidental initiation of the containment spray system, while reactor is in full power, could have severe consequences. If the relatively cold water suddenly cools down the wall of fully pressurized reactor pressure vessel, the induced thermal stresses might damage the pressure vessel wall. To find out how the pressure vessel wall cools down, input data on heat transfer is required. Heat transfer from the pressure vessel wall to the water was studied experimentally to determine the heat transfer coefficients for further calculations. A test facility was built to study this problem and several tests were conducted to define the effects of different parameters on heat transfer.

According to the results in this study the applied correlations failed in estimating the heat transfer coefficient in the first few minutes of the cooling transient. The effect of bubble boiling is not taken into account in the correlations. In the later phase of the cooling transient, natural convection correlation give the most accurate approximation while the forced convection correlations fail to estimate the heat transfer coefficient. The example in section 5 illustrates only the early phase of the cooling transient. However, the most important phase of the transient in the point of view of PTS is later phase of the cooling transient. It is obvious that a single correlation applied in this study cannot handle the entire range of heat transfer types during this kind of cooling transient. The Churchill & Chu correlation provides a good estimate of the steady state heat transfer coefficient, but another correlation is necessary at least for the boiling stage of the transient.

This experimental work together with the numerical methods used in the study provided data for further mechanical analyses.

References

[1] M. Krishnan and D.G.R. Sharma, “Determination of interfacial heat transfer coefficient h in unidirectional heat flow by Beck’s non linear estimation procedure”, Int. Comm. Heat mass transfer, vol. 23, p. 203-214, 1996.

[2] J.V. Beck and B. Blackwell, “Comparison of some inverse heat conduction methods using experimental data”, Int. J. Heat mass transfer, Vol. 39. p. 3649-3657, 1996.

[3] S.W. Churchill and H.H.S. Chu, “Correlating equations for laminar and turbulent free convection from a vertical plate”, Int. J. Heat mass transfer, vol. 18, p.1323-1329, 1975.